J Electr Eng Technol.2018; 13(?): 1921-718
http://doi.org/10.???/JEET.2018.13.2.1921

ISSN(Print) 1975-0102
ISSN(Online) 2093-7423

Design and Fabrication of a Compact Passive Lowpass Filter with Very Ultra Wide Stopband

Gholamhosein Moloudian* and Massoud Dousti†

Abstract – Microstrip lowpass filters (LPFs) with good performance are used in most tele-communication systems. The important features of a LPF include wide stopband and high figure of merit. In this study, a resonator was used to design a LPF. Three suppression cells were also used to widen the stopband by up to 40 GHz. The filter cut-off frequency is equal to 1.2 GHz. The results show that the stopband width, with consideration of -30 dB attenuation, is equal to 34.2 GHz and its figure-of-merit is equal to 34620. The simulated, measured and LC equivalent circuit results of the proposed LPF are in good agreement and the filter dimensions were equal to $0.11\times0.08\ \lambda g^2$.

Keywords: Lowpass filter, Stopband, Compact, Microstrip

1. Introduction

In most telecommunication and communication systems, LPFs are widely used to remove unwanted signals. Reference [1] deals with improvement of LPF parameters and includes all regulations associated with filter design. The most important parameters of a LPF include the following: small size, wide stopband, sharp frequency response from the pass to stop mode and high figure of merit (FOM). Different resonators can be used to design a LPF. Some examples of such resonators are described below. A LPF with good suppression factor (SF) using suspended substrate microstrip lines (SSMLs) is presented in [2], but the stopband is small and sharp roll-off rate (ROF or ζ) of the frequency response is not suitable. In [3], hairpin resonators were used to design LPF. In the stopband, the -20dB suppression ranges from a frequency of 1.9 to 15 GHz. In [4] a hairpin resonator with two open stubs and one spiral slot is for designing a LPF. The filter's cut-off frequency is equal to 2 GHz and its SF in the stopband is equal to -10 dB. The disadvantage of this filter can be cited the low SF and low FOM. An ultra-wide stopband LPF using multimode resonators is presented in [5], but the sharpness of the frequency response, SF and FOM parameters are not suitable. A compact LPF with ultra-wide stopband characteristic is presented in [6], but the ROF is bad. Defected ground structure (DGS) can also be used to design a LPF. In [7], a DGS-based LPF with proper functioning is provided. In [8], developed an approach to design of aperiodic stubs on a microstrip line. A compact LPF with a meander line, a coupled line and two open stubs is presented in [9], but the SF is low. A compact LPF with good return loss (RL) in the passband is presented in [12], but the FOM of the frequency response and FOM are not suitable. In recent years, various resonators with different geometries and structures such as quasi-elliptic [10], Windmill resonator [11], meandered-slot dumbbell resonator [13], and artificial transmission lines [14] were offered to produce compact LPF.

In this paper, a compact microstrip LPF with sharp roll-off rate (ROF or ζ), and very ultra-wide stopband is presented. The proposed LPF is designed, simulated and fabricated. The benefits of this article can be used to proposed LC equivalent circuit for the LPF. The simulated, measured and LC equivalent circuit results of the proposed LPF are in good agreement. The paper is organized as follows: in Section 2, the proposed resonator and suppression cells (layout, LC equivalent circuit, frequency response, and ABCD parameters) with very good performance is presented. In Section 3, the proposed LPF has been fabricated and measured. Some conclusion remarks are presented in Section 4.

2. Resonator Analysis and Filter Design

Fig. 1 shows the topology, synthesis and analysis of a proposed radial stub resonator (original resonator). The proposed resonator acts like a third-order Chebyshev LPF. This resonator behaves like a LPF. Third-order Chebyshev LPF, LC equivalent circuit of this resonator and simulations (LC and EM) can be seen in Fig. 1. The coefficients for this filter f=1.2 GHz, IL (dB)=0.1, N=3, $g_0=g_4=1$, $g_{L1}=1.202$, $g_{L2}=0.1614$, $g_{C2}=1.255$, $g_{L3}=1.604$. We use the following relationships to calculate the inductors and capacitors.Using the following relationships, the values of the inductors and capacitors of the LPF can be obtained [1].

† Corresponding Author: Department of Electrical and Computer Engineering, Science and Research Branch, Islamic Azad University, Tehran, Iran. (m_dousti@srbiau.ac.ir)
* Department of Electrical Engineering, Arak Branch, Islamic Azad University, Arak, Iran. (gh-moloudian92@iau-arak.ac.ir)
Received: July 27, 2017; Accepted: December 26, 2017

$$L_i = \frac{1}{2\pi f_c} Z_0 g_{Li} \quad (1)$$

$$C_i = \frac{1}{2\pi f_c} \frac{1}{Z_0} g_{Ci} \quad (2)$$

$$l_{Li} = \frac{\lambda_{gLi}}{2\pi} Sin^{-1}\left(\frac{2\pi f_C L_i}{Z_{0L}}\right) \quad (3)$$

$$l_{Ci} = \frac{\lambda_{gCi}}{2\pi} Sin^{-1}\left(2\pi f_C C_i Z_{0C}\right) \quad (4)$$

Finally, the values for inductors: W=0.1, l_{L1}=13.7, l_{L3}=15.2, l_{L2}=13.7 and for capacitors: W=4, l_{C2}=9.4 are obtained (mm).

In the three case, a transmission zero near 2 GHz is created. The dimensions of the proposed layout as shown in Fig. 1 are a=4.8 mm, b=4.9 mm, R=4 mm, and p=5.2 mm. In Fig. 1, L_a is the inductance of the line with length of a, L_b is the inductance of the line with length of b, L_p is the inductance of the line with length of p, and C_R is the capacitance of semi-circular cell with respect to the ground. Using the electromagnetic (EM) simulator of advanced design system (ADS) software, these values were calculated through optimization processes. The inductance and capacitance values of LC equivalent circuit for the original resonator are L_a=0.5 nH, L_b=4.64 nH, C_R= 1.65 pF, and L_p=4.36 nH. The ABCD parameters of the proposed resonator is obtained as:

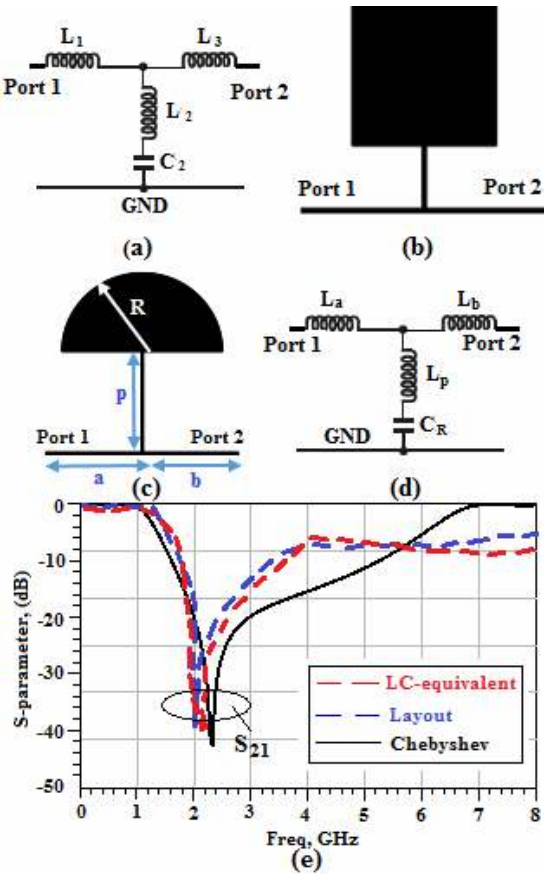

Fig. 1. Resonator, (a) third-order Chebyshev, (b) layout, (c) proposed resonator, (d) LC equivalent circuit and (c) simulations results

$$A = \frac{1-\omega^2 C_R (L_a + L_p}{1-\omega^2 C_R L_p} \quad (5)$$

$$B = \frac{j\omega^3 C_R L_p L_b - j\omega\left(L_b + L_a\right) + j\omega^3 C_R L_a \left(L_p + L_b\right)}{1-\omega^2 C_R L_p} \quad (6)$$

$$C = \frac{j\omega C_R}{1-\omega^2 C_R L_p} \quad (7)$$

$$D = \frac{1-\omega^2 C_R \left(L_b + L_p\right)}{1-\omega^2 C_R L_p} \quad (8)$$

$$\text{ABCD} = \begin{bmatrix} A & B \\ C & D \end{bmatrix} \quad (9)$$

The relationship between insertion loss (S_{21} parameter) and ABCD parameters is:

$$S_{21} = \frac{2Z_0 \left(-\omega^2 C_R L_p\right)}{Z_0 K_1 + K + K_2} \quad (10)$$

$$K_1 = \left[2 - \omega^2 C_R \left(L_a + L_b + 2L_p\right)\right] \quad (11)$$

$$K_2 = j\omega^3 C_R \left(L_p L_b + L_a L_p + L_a L_b\right) \quad (12)$$

$$K_3 = j\omega\left(C_R - L_b - L_a\right) \quad (13)$$

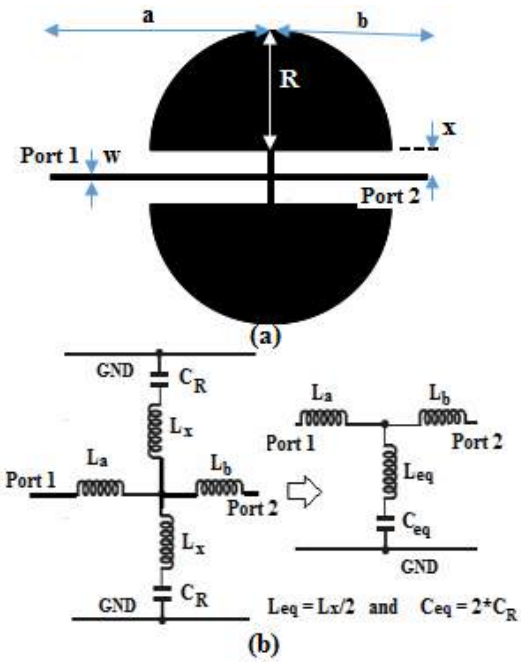

Fig. 2. Suppression cell, (a) layout and (b) LC equivalent circuit

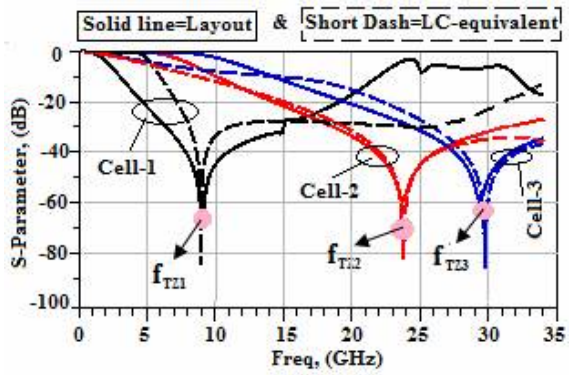

Fig. 3. Simulations (LC and EM) of three suppressor cells

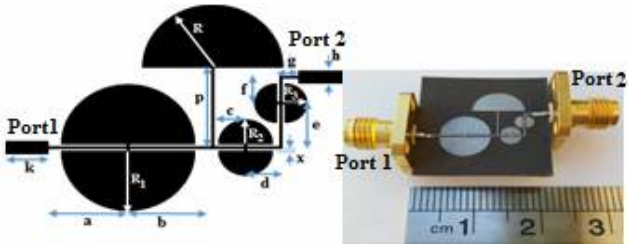

(a) (b)

Fig. 4. The proposed LPF (a) layout, and (b) fabricated.

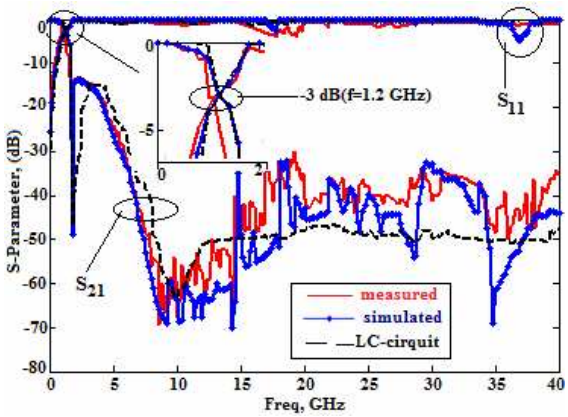

Fig. 5. Simulated, measured and LC equivalent circuit results of the proposed filter

According to equation 10, by adjusting the L_P and C_R values can be controlled transmission zero. The suppression cells provided below were used to improve the performance of the proposed resonator's S_{21} parameters in the stopband. The proposed structure of suppression cells together with its equivalent circuit are presented in Fig. 2.

Fig. 2 shows the layout and LC equivalent circuit for the suppressor cell. In Fig. 2, L_a is the inductance of the line with length of a, L_b is the inductance of the line with length of b, L_x is the inductance of the line with length of x, and C_R is the capacitance of radial stub cell with respect to the ground. Due to the symmetry of the proposed equivalent circuit can be simplified. Given that we have two parallel branches of L_x and C_R, so as to simplify can act as $L_{eq}=L_x/2$, $C_{eq}=2\times C_R$. Here, the three suppression cells provided in Fig. 3 were used. The S_{21} scattering parameter for each suppression cell, together with their equivalent circuit response, are provided in this figure.

Suppressing cells makes use of three transmission zeros (f_{TZ1}, f_{TZ2} and f_{TZ3}) at frequencies near 9 GHz, 24 GHz and 30 GHz be created (conforms to the Fig. 3). The use of suppression cells improves insertion loss in the stopband. The dimensions of the proposed layout as shown in Fig. 3 are for cell-1: a_1=4.6 mm, b_1=4.7 mm, R_1=3.8 mm, x_1=0.2 mm, for cell-2: a_2=1.8 mm, b_2=1.85 mm, R_2=1.5 mm, x_2= 0.2 mm, and for cell-3: a_3=1.6 mm, b_3=1.65 mm, R_3=1.2 mm, x_3=0.2 mm. The inductance and capacitance values of LC equivalent circuit for the suppressor cells are L_{a1}=2.5 nH, L_{b1}=2.5 nH, L_{eq1}=0.49 nH, C_{eq1}=0.65 pF, L_{a2}= 0.16 nH, L_{b2}=4.9 nH, L_{eq2}=0.16 nH, C_{eq2}=0.28 pF, L_{a3}=3.9 nH, L_{b3}=0.37 nH, L_{eq3}=0.26 nH, C_{eq3}=0.11 pF. The results of proposed LC equivalent circuit are in good agreement with the layout results. Using the ADS software, these values were calculated through optimization processes.

3. The Proposed Filter Structure

The proposed filter consists of a main resonator with three suppression cells for improving the S_{21} parameter in the stopband. Fig. 4 presents the proposed filter. The characteristic impedance of ports 1 and 2 are 50 Ω, and the SMA connector is used. The dimensions of the proposed layout as shown in Fig. 4 are a=4.6 mm, b=4.8 mm, c=1.8 mm, d=1.94 mm, e=2.8 mm, f=1.6 mm, g=1 mm, k=2.5 mm, p=5.2 mm, h=0.78 mm, R=4 mm, R_1=3.8 mm, R_2=1.5 mm, R_3=1.2 mm, and x=0.2 mm. The proposed filter was developed on the RT/Duroid 5880 substrate with a thickness of 10 mil (0.254 mm), dielectric constant of 2.2 and loss tangent of 0.0009. Fig. 5 shows the scattering parameter of the filter. The simulated, measured and LC equivalent circuit results of the proposed LPF are in good agreement. The results show that the proposed LPF has a -3 dB cutoff frequency at 1.2 GHz. As shown in Fig. 5, the proposed LPF has an ultra-wide stopband from 5.8 to 40 GHz with consideration of -30 dB attenuation level.

Fig. 6(a) shows the LC equivalent circuit of the proposed LPF while Fig. 6(b) shows the simplified LC equivalent circuit of the proposed LPF. Due to the symmetry in some parts of the proposed circuit can be simplified. Given that we have some parallel branches of L_{xi} and C_{Ri}, so as to simplify can act as $L_{eqi}=L_{xi}/2$, $C_{eqi}=2\times C_{Ri}$, (i=1, 2, 3). After simplification, the equivalent circuit in Fig. 6(b) is proposed. The inductance and capacitance values of the simplified LC equivalent circuit for the proposed LPF are L_a=2 nH, L_b=1.2 nH, L_c=2.25 nH, L_d=0.4 nH, L_e=0.8 nH, L_f=1 nH, L_g=1.5 nH, L_{eq1}=0.25 nH, C_{eq1}=1 pF, L_p=5 nH, C_R=1.4 pF, L_{eq2}=2.9 nH, C_{eq2}=2 pF, L_{eq3}=5 nH, and C_{eq3}=1.5 pF. Table 1 compares the performance of the proposed LPF with the results of other

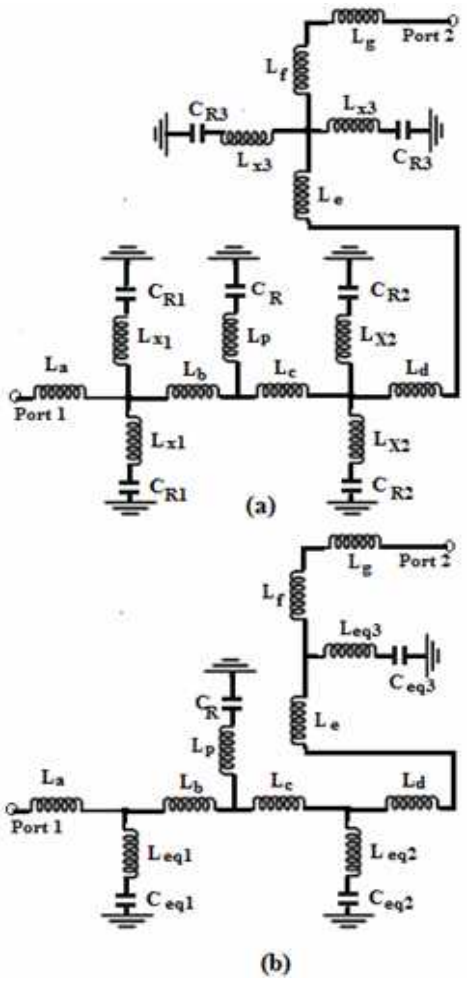

Fig. 6. (a)The LC equivalent circuit of the proposed LPF, and (b) the simplified LC equivalent circuit of the proposed LPF

Table 1. Performance comparisons of the proposed LPF with other works

Refs.	fc (GHz)	ROF (dB/GHz)	RSB	SF	NCS	BW stop	FOM
[2]	1	35.6	1.47	3	0.0227	9.79	6826
[3]	1.6	52.8	1.53	2	0.0091	14.2	17652
[4]	2	43.9	1.63	1	0.0151	17	4741
[5]	1.8	---	1.58	1.5	0.0099	21.2	---
[6]	1.74	20.5	1.59	2	0.0204	20.2	3196
[8]	1.9	37	1.45	1.8	0.0920	6	1050
[9]	1.2	24	1.38	1.5	0.0088	8.44	5281
[10]	1.18	36	1.32	1.5	0.0064	7.04	11543
[11]	1.76	51.5	1.56	2	0.0475	10.2	3383
[12]	2.4	15.9	1.04	2	0.1056	7.5	314
[13]	2.2	58.6	1.73	2	0.0555	25.7	3654
This work	1.2	68	1.49	3	0.0088	34.2	34620

$\xi = (\alpha_{max}-\alpha_{min}) / (fs - fc)$; SF = ((max attenuation level in stopband) / 10);
RSB=Stopband bandwidth/Stopband center freq;
NCS = Physical size / λg^2; FOM = (ξ ×RSB × SF)/(NCS × AF)

works. In this Table, the ROF or ζ is a roll-off rate, relative stopband bandwidth (RSB), suppression factor (SF), normalized circuit size (NCS), and figure-of merit (FOM) are defined as in [10].

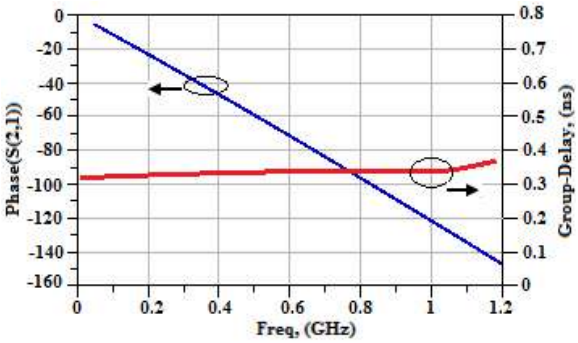

Fig. 7. Phase and group delay for the proposed LPF in the passband

According to the results obtained for the proposed LPF, the -3 dB cut-off frequency is 1.2 GHz. Insertion loss in the passband is less than 0.4 dB. The ROF parameter shows the slope of frequency response curve of the passing to stop. The proposed LPF has a sharp roll-off rate of 68 dB/GHz. The insertion loss in the stopband is more than 30 dB, which increases the SF parameter up to 3. The size of the proposed LPF is 0.11λg × 0.08λg where, λg is the guided wave length at the cut-off frequency. The proposed LPF has an ultra-high FOM of 34620 which shows the performance of the proposed filter is appropriate. The advantages of this filter can be noted the ultra-wide stopband (equal to 34.2 GHz). The simulation results for the layout and proposed LC equivalent circuit are in good agreement with the measured of the fabricated sample. Phase and group delay for proposed filter in the passband shown in Fig. 7. As seen in Fig. 7, the flat group delay is achieved in the pass band zone with range of variation 0.32-0.37 ns for the proposed LPF. The phase of the insertion loss is linear, which indicates the good performance for the proposed LPF.

4. Conclusion

In this study, a resonator with three suppression cells were used to design a LPF with an ultra-wide stopband of about 34.2 GHz. The filter is very small in size and its other parameters are favorable as well. Suppression in the stopband is equal to -30 dB. It was found that the simulated, measured and LC equivalent circuit results of the proposed LPF are in good agreement. The proposed filter's figure of merit is very high and equal to 34620. The proposed filter can be used in telecommunication systems.

References

[1] J.-S. Hong, and M. J. Lancaster, "Microstrip filters for RF/microwave applications," Wiley, New York. 2001.

[2] X. Feng, Y. Zhang, G. Zhu, Y. Fan, W.T. Joines, and Q. H. Liu, "Design of LPF using suspended substrate microstrip lines as High-Z sections for stopband extension," *Microw. Optical Technol. Lett.*, vol. 58, no. 5, pp. 1204-1207, May 2016.

[3] S. Liu, J. Xu, and Z. Xu, "Compact lowpass filter with wide stopband using stepped impedance hairpin units," *Electron. Lett.*, vol. 51, no. 1, pp. 67-69, January 2015.

[4] F. Wei, L. Chen, and X.-W. Shi, "Compact lowpass filter based on coupled-line hairpin unit," *Electron. Lett.,* vol. 48, no. 8, pp.379-381, March 2012.

[5] Q. Li, Y. Zhang, and Y. Fan, "Compact ultra-wide stopband low pass filter using multimode resonators," *Electron. Lett.,* vol. 51, no. 14, pp. 1084-1085, July 2015.

[6] S.-W. Lan, M.-H. Weng, S.-J. Chang, and C.-Y. Hung, "A compact low-pass filter with ultrabroad stopband characteristics," *Microw. Optical Technol. Lett.,* vol. 57, no. 12, pp. 2800-2803, December 2015.

[7] F.-C. Chen, H.-T. Hu, J.-M. Qiu, and Q.X. Chu, "High selectivity low-pass filters with ultrawide stopband based on defected ground structures," *IEEE Trans. Compon. Pack. Manuf. Technol.,* vol. 5, no. 9, pp. 1313-1319, August 2015.

[8] C.-H. Chen, "Design of artificial transmission line and low-pass filter based on aperiodic stubs on a microstrip line," *IEEE Trans. Compon. Pack. Manuf. Technol.,* vol. 4, no. , pp. 922-928, May 2014.

[9] X. Chen, L. Zhang, Y. Peng, Y. Leng, H. Lu, and Z. Zheng, "Compact lowpass filter with wide stopband bandwidth," *Microw. Optical Technol. Lett.,* vol. 57, no. 2, pp.367-371, February 2015.

[10] J. Wang, L.-J. Xu, S. Zhao, Y.-X. Guo, and W. Wu, "Compact quasi-elliptic microstrip lowpass filter with wide stopband," *Electron. Lett.,* vol. 46, no. 20, pp. 1384-1385, September 2010.

[11] H. Cao, W. Ying, H. Li, and S. Yang, "Compact lowpass filter with wide stopband using novel Windmill resonator," *J. Electromagn. Waves Appl.,* vol. 26, no. 17-18, pp. 2234-2241, December 2012.

[12] A. Boutejdar, A. Omar, and E. Burte, "High performance wide stop band low pass filter using a vertically coupled DGS/DMS resonators and inter-digital capacitor," *Microw. Optical Technol. Lett.,* vol. 56, no. 1, pp. 87-92, January 2014.

[13] H. L. Cao, W. B. Ying, H. Li, and S. Z. Yang, "Compact lowpass filter with ultra-wide stopband rejection using meandered-slot dumbbell resonator," *J. Electromagn. Waves Appl.,* vol. 26, no. 17-18, pp. 2203-2210, December 2012.

[14] Y. He, X. Wu, and C.-J. Liu, "Novel miniaturized low-pass filters from artificial transmission line structures," *J. Electromagn. Waves Appl.,* vol. 28, no. 10, pp. 1269-1274, May 2014.

Gholamhosein Moloudian was born in Kazerun, Iran in 1988. He received the associate's degree in electronics from Technical and Vocational College of Yasouj (Yasouj, Iran in 2008), the B.Sc. degree in Electronics from Higher Education Center of Shiraz (Shiraz, Iran in 2010), the M.Sc. degree in Electronics from Islamic Azad University of Bushehr (Bushehr, Iran in 2012), and the Ph.D. degree in Electrical Engineering (Electronics) from Islamic Azad University of Arak (Arak, Iran in January 2018). His research interests include design and analysis of microwave/RF circuits, RF MEMS, Neuro-Fuzzy algorithms, tunable microstrip and optical devices (filter, diplexer, and antenna).

Massoud Dousti received B.S. in Electrical Engineering from Orleans University, Orleans, France and M.S. degrees in Electronics (Microwave and Optics) from Limoges University, Limoges, France, in 1991 and 1994 and Ph.D. in Electronics (Active Microwave Circuits) from University of Paris VI, Pierre et Marie Currie, in 1999 respectively. He served as a teaching assistant in the Department of Electrical Engineering at Ensea, Cergy Pontoise, France from 1998 to 2000. In 2001 he joined Department of Electrical and Computer Engineering of Science and Research branch, Islamic Azad University, Tehran, IRAN, where he is now an Associate Professor. His research interests are linear and non-linear microwave/RF circuits and systems design, millimeter wave circuits design, and MMIC technology.